CALIBRATION OF PHOTOVOLTAIC MODULE PERFORMANCE MODELS USING MONITORED SYSTEM DATA

Clifford W. Hansen[1a], Katherine A. Klise[1b], Joshua S. Stein[1c], Yuzuru Ueda[2], Keiichiro Hakuta[3]
[1a] Sandia National Laboratories, PO Box 5800, Albuquerque, NM 87185, USA, cwhanse@sandia.gov, 505-284-1643
[1b] kaklise@sandia.gov, [1c] jsstein@sandia.gov,
[2] Tokyo Institute of Technology, Tokyo, Japan, ueda.y.ae@m.titech.ac.jp
[3] NTT Facilities Inc, Tokyo, Japan, hakuta22@ntt-f.co.jp

ABSTRACT: Calibration of a photovoltaic module performance model currently relies on measurements of electrical output taken with the module outdoors on a two-axis tracker, or indoors using a solar simulator. These measurements require expensive infrastructure. By contrast, measuring electrical performance for systems outdoors on fixed racking is substantially cheaper, yet no method currently exists to translate these meaurements to model coefficients. We present and validate methods to calibrate the Sandia Photovoltaic Array Performance Model and the California Energy Commission model using data collected outdoors for modules at fixed tilt orientation. A method to successfully calibrate module performance models without recourse to a two-axis tracker or a solar simulator expands the ability to rapidly characterize photovoltaic modules in actual operating conditions.
Keywords: Photovoltaic, System performance, Modelling

1 INTRODUCTION

Performance models for photovoltaic (PV) systems predict system output over ranges of irradiance and temperature. Two popular performance models are the Sandia Photovoltaic Array Performance Model (SAPM) [1], which comprises a set of empirical expressions for short-circuit current, open circuit voltage, and the maximum power point, and the California Energy Commission (CEC) model [2], which models a module as a single diode equivalent circuit. The popular software package PVsyst [3] also represents a PV module as a single diode equivalent circuit albeit with some differences in its mathematical model.

Each model requires a set of coefficients which are specific to the module being considered. In addition, both models include terms which adjust the incident irradiance to account for reflection losses at the module surface when the module is not normal to the sun, and for variation in the spectral content of incident irradiance, as well as other loss factors such as soiling.

Accurate module performance models are essential to the economic and technical success of a PV power system. Calibration of these models is usually achieved by measuring module performance (i.e., IV curves) outdoors on a two-axis tracker [4] or indoors using a solar simulator [5]. Methods are available to determine the required model coefficients from such data [4, 6, 7].

By contrast, no validated methods are available to determine performance model coefficients using data from a monitored system, i.e., from I-V curves measured periodically with concurrent irradiance and temperature measurements for a module outdoors at fixed tilt orientation. In this paper, we present and validate techniques to calibrate the SAPM and CEC model using data from a monitored system. These techniques open the possibility to dramatically reduce the cost of the equipment required to accurately calibrate performance models, and also may provide a method to calibrate a performance model descriptive of an already-built PV system.

2. PERFORMANCE MODELS

Two performance models are used in this study: the SAPM and the CEC model. In the model descriptions that follow, current is in Amps, voltage is in Volts, power is in Watts, irradiance is in Watts/m^2, temperature is in degrees Celsius, and resistance is in Ohms. Temperature coefficients are in Amps/C or Volts/C unless otherwise noted.

2.1 The Sandia Array Performance Model

The SAPM comprises the following equations:

$$E_e = f_1(AM_a)\left(E_b f_2(AOI) + E_{diff} f_d\right) / E_0 \quad (1)$$

$$I_{SC} = I_{ISC0} E_e \left(1 + \alpha_{ISC}\left(T_C - T_0\right)\right) \quad (2)$$

$$V_{OC} = V_{OC0} + nN_S\delta\left(T_C\right)\ln\left(E_e\right) + \beta_{VOC}\left(T_C - T_0\right) \quad (3)$$

$$I_{MP} = I_{MP0}\left(C_0 E_e + C_1 E_e^2\right)\left(1 + \alpha_{IMP}\left(T_C - T_0\right)\right) \quad (4)$$

$$V_{MP} = V_{MP0} + C_2 nN_S\delta\left(T_C\right)\ln\left(E_e\right) + C_3 N_S\left(n\delta\left(T_C\right)\ln\left(E_e\right)\right)^2 + \beta_{VMP}\left(T_C - T_0\right) \quad (5)$$

Short-circuit current (I_{SC}), current at the maximum power point (I_{MP}), open circuit voltage (V_{OC}), voltage at the maximum power point (V_{MP}), and the maximum power point (P_{MP}) have the usual meanings as do temperature coefficients (α_{ISC}, α_{IMP}, β_{VOC}, and β_{VMP}). For the SAPM, α_{ISC} and α_{IMP} are in units of 1/C. The subscript '0' indicates a value at standard test conditions (STC) irradiance (E_0 = 1000 W/m^2), reference cell temperature (T_0 = 25°C), and reference solar spectrum.

E_e is the effective irradiance that can be converted to electricity, E_b is the beam component of incident irradiance, and E_{diff} is the diffuse component of incident irradiance. The variables AM_a and AOI are apparent air mass and angle of incidence, respectively. The term f_1 is normally a polynomial in AM_a that accounts for the influence of solar spectrum on I_{SC}, the term f_2 quantifies the fraction of beam irradiance that is not reflected from the module's face, and f_d is the fraction of diffuse irradiance used by module. The coefficients C_0, C_1, C_2, and C_3 relate I_{MP} and V_{MP} to effective irradiance. N_S is the number of cells in series, n is the diode (ideality) factor, and T_C is the cell temperature averaged over the

module's cells. The term $\delta(T_C)$ is the cell thermal voltage defined as $(k \times T_C)/q$ where k is Boltzmann's constant, 1.38×10^{-23} J/K and q is the elementary charge, 1.62×10^{-19} C.

2.2 The California Energy Commission Model

The CEC model comprises the following equations:

$$I = I_L - I_O\left[\exp\left(\frac{V+IR_S}{nN_S\delta(T_C)}\right)-1\right]-\frac{V+IR_S}{R_{SH}} \quad (6)$$

$$I_L = I_L\left(E,T_C\right) = \frac{E}{E_0}\frac{M}{M_0}\left[I_{L0}+\alpha_{ISC}\left(T_C-T_0\right)\right] \quad (7)$$

$$I_O = I_{O0}\left[\frac{T_C}{T_0}\right]^3 \exp\left[\frac{1}{k}\left(\frac{E_g\left(T_0\right)}{T_0}-\frac{E_g\left(T_C\right)}{T_C}\right)\right] \quad (8)$$

$$E_g\left(T_C\right) = E_{g0}\left(1-0.0002677\left(T_C-T_0\right)\right) \quad (9)$$

$$R_{SH} = R_{SH0}\left(E_0/E\right),\ R_S = R_{S0} \quad (10)$$

In the CEC model, I and V are the current and voltage along an IV curve, and T_C is the cell temperature. I_L is the light current, I_O is the diode reverse saturation current, E_g is the band gap, R_{SH} is shunt resistance, and R_S is series resistance. The values of these quantities at STC are I_{L0}, I_{O0}, E_{g0}, R_{SH0} and R_{S0}. E is the incident irradiance reaching the PV cell (i.e., plane of array irradiance reduced by reflection losses). M/M_0 is termed the airmass modifier and accounts for the effect of solar spectrum on I_{SC} and is equivalent to $f_1(AM_a)$ in SAPM [2]. N_S, n, $\delta(T_C)$, E_0, and T_0 have the same definitions as noted for the SAPM. The temperature coefficient α_{ISC} is in units of A/C.

3 MONITORED SYSTEM DATA

Data collected from five PV modules were used to calibrate performance models using fixed-tilt data. The modules are located at Los Alamos, New Mexico, USA and represent a range of technologies (Table I). IV curves, POA irradiance, global horizontal irradiance (GHI), direct normal irradiance (DNI), and module back-surface temperature (T_M) were measured every 5 minutes between January and September 2013 by NEDO. Data sets for each module contain over 44,000 individual IV curves.

Table I: Photovoltaic modules considered

	Cells	Nameplate P_{MP} (W)
Sharp mono-Si	60	240
Sunpower mono-Si	72	240
Kyocera poly-Si	60	235
Kaneka tandem a-Si	106	110
Solar Frontier CIS	109	85

Although GHI and DNI measurements are available, we chose to use only POA irradiance measurements for model calibration in order that our methods could be broadly applicable. I_{SC}, I_{MP}, V_{OC}, V_{MP}, and P_{MP} are extracted from each IV curve. AM_a and AOI are computed using the module's orientation and solar ephemerides.

Before using the data to calibrate the performance models, several filters are applied to eliminate erroneous or inconsistent data. These filters include (1) removing data with physically unreasonable values, (2) removing data with high AM_a or AOI because measurements at these conditions are generally less reliable, and (3) removing data when the POA irradiance and I_{SC} are not linearly correlated (Fig. 1). When data meets any of these criteria, all measurements at that time are eliminated from the calibration procedure. After filtering, the data is divided into in-sample and out-of-sample subsets of roughly equal size using a random selection of the dataset. The in-sample data set is used to calibrate the model. The out-of-sample data set is used for model validation.

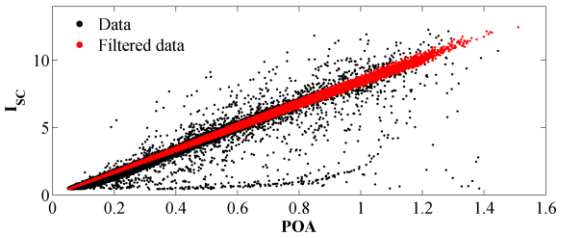

Figure 1: Filtering for mismatched IV curves and irradiance measurements for the Sharp mono-Si module.

4 CALIBRATION METHODS

Temperature coefficients (i.e., α_{ISC}, α_{IMP}, β_{VOC}, and β_{VMP}) cannot be determined from monitored system data, because measurement of these coefficients requires measuring module electrical output with relatively constant irradiance while module temperature changes. Typically, these coefficients are determined either indoors using a temperature controlled flash tester, or are measured outdoors by shading the module until its temperature equilibrates with ambient air temperature, then exposing the module and measuring electrical output while the module warms. Equivalent conditions do not exist when a system is being monitored outdoors. For this study, it is assumed that temperature coefficients given in data sheets are sufficiently accurate.

Cell temperature, T_C, is not measured directly on the monitored systems. Rather, module back-surface temperature, T_M, is measured by thermocouples. Cell temperature is estimated as

$$T_C = T_M + 3\frac{POA}{E_0} \quad (11)$$

where POA in Eq. 11 is the measured POA irradiance. The constant 3°C in Eq. 11 is representative of the difference between back-surface and cell temperatures in flat-plate crystalline silicon modules [1].

When calibrating the SAPM and the CEC models using fixed tilt data, the primary challenge is establishing a relationship between POA irradiance and I_{SC} for the SAPM and between POA irradiance and the light current I_L for the CEC model. For the SAPM, POA irradiance must be separated into its beam and diffuse components (E_b and E_{diff}, respectively), and the influence of solar spectrum and reflection losses must be estimated, as indicated in Eq. 1. For the CEC model, POA irradiance is used directly to estimate the incident irradiance reaching the PV cell, E in Eq. 7. This assumption is reasonable except at very high AOI.

The SAPM and CEC model use the same methods to estimate the airmass modifier ($f_1(AM_a)$ in Eq. 1 and M/M_0 in Eq. 7). Eq. 1 is used to estimate $f_1(AM_a)$ using measurements made during clear-sky conditions. The clear sky conditions are necessary to estimate E_b and E_{diff} in Eq. 1. To identify clear sky conditions using only POA irradiance measurements, the Haurwitz clear sky model [8] was used to estimate clear sky GHI, the DIRINT modification of the DISC model [9] was used to estimate clear sky DNI, the Sandia's Simple Sky Diffuse Model [10] was used to estimate diffuse irradiance, and the ground diffuse model in [11] was used to estimate ground diffuse irradiance. The selected models are able to predict clear-sky irradiance quantities with reasonable accuracy [12]. These quantities are combined to obtain a modeled value for POA irradiance under clear sky conditions.

The POA measurements are compared to the modeled values to select data that are within 100 W/m^2 of the corresponding modeled values. Clear sky measurements comprise approximately 50% of the data for each module. Fig. 2 illustrates the POA data and the data that is within 100 W/m^2 of the POA irradiance under clear sky conditions from the Solar Frontier module. This figure includes all POA monitored data, plotted as a function of solar time.

Using the clear-sky data, E_b and E_{diff} in Eq. 1 are then estimated from the measured POA irradiance data. When a two-axis tracker is available, E_b can be computed directly from DNI measured using a pyrheliometer. Using the measured POA irradiance under these identified clear sky conditions, E_b and E_{diff} were estimated as 85% and 15% of the measured POA value, respectively. Many clear sky models (e.g., [13]) assume similar proportions for beam and sky diffuse irradiance under clear sky conditions and the contribution to E_{diff} from ground reflections can be assumed to be negligible.

Estimates for f_d and the $f_2(AOI)$ function are set based on measured values for other, similar modules. Since only flat plate modules are considered, we set f_d = 1 which is typical for modules that have a high transmission of light through the front surface. The influence of AOI was estimated using $f_2(AOI)$ defined by [14] using an angular loss coefficient of 0.17.

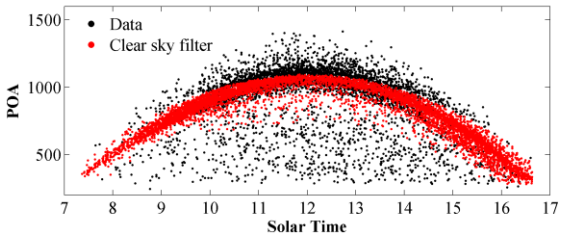

Figure 2: Clear sky filter on POA used to estimate parameters in Eq. 1.

I_{SC0} and $f_1(AM_a)$ can then be estimated by substituting Eq. 1 into Eq. 2, and performing a regression between $I_{SC}/(E_b \times f_2(AOI)+f_d \times E_{diff})(1+\alpha_{ISC}(T_C-T_0))$ and AM_a. A quadratic in AM_a is first fit to the data where 1 < AM < 2 and the value of I_{SC0} is taken to be the value of the fitted quadratic at AM_a = 1.5 because, by convention, $f_1(AM_a = 1.5)=1$. With I_{SC0} in hand, $f_1(AM_a)$ is estimated by regressing $I_{SC}/I_{SC0}(E_b \times f_2(AOI)+f_d \times E_{diff})(1+\alpha_{ISC}(T_C-T_0))$ onto AM_a using all data during clear sky conditions.

Fig. 3 shows the computed values of $f_1(AM_a)$ and the values used for the regression for the Kyocera poly-Si module data. In the figure, each data point is colored according to the solar time of the measurement, which illustrates that I_{SC} is higher in the early morning due to red-shifted solar spectrum. The other 4 modules show similar patterns. These patterns are also observed in data measured at Sandia National Laboratories in Albuquerque, NM, USA, using a two-axis tracker, indicating that the method presented here for isolating spectrum effects in the fixed-tilt data is yielding reasonable results. However, we note that the dispersion in Fig. 2 is roughly twice that observed in data measured using a two-axis tracker. The greater dispersion likely results from the use of modeled rather than measured direct and diffuse irradiance. The $f_1(AM_a)$ air mass modifier is used in both the SAPM ($f_1(AM_a)$ in Eq. 1) and CEC model (M/M_0 in Eq. 7).

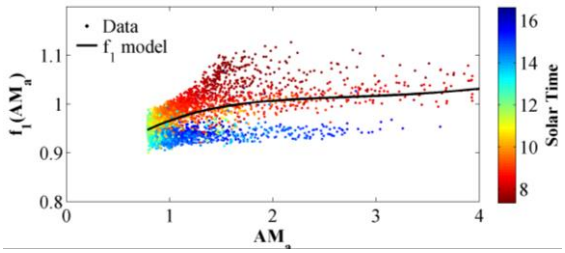

Figure 3: Empirical function representing effect of spectral content on I_{SC} for the Kyocera poly-Si module. Each point on the graph is colored according to the solar time of the measurement.

The SAPM and CEC model calibrations also use the same method to estimate the diode factor n. The diode factor is estimated from the relationship between V_{OC} and E_e in Eq. 3 of the SAPM, which can be shown to be approximately the same as Eq. 6 in the CEC model evaluated at open-circuit conditions. The diode factor n can therefore be estimated by linear regression between V_{OC}-$\beta_{VOC} \times (T_C-T_0)$ and $N_S \times \delta(T_C) \times \ln(E_e)$. For the SAPM, V_{OC0} is estimated from the intercept of this line. An example fit is shown in Fig. 4.

At this point, there are 6 parameters left to estimate in the SAPM: I_{MP0}, V_{MP0}, C_0, C_1, C_2, and C_3. These parameters can be estimated by rearranging Eq. 4 and 5 and fitting a quadratic model to each using regression techniques.

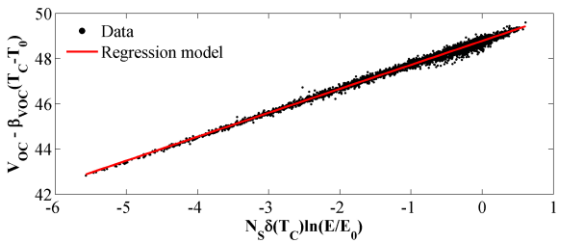

Figure 4: Regression model for the diode factor, n, for the Sunpower mono-Si module.

For the CEC model, we set the airmass modifier M/M_0 equal to $f_1(AM_a)$ as estimated for the SAPM and estimate the diode factor n in the same manner as for SAPM. There remain five parameters yet to estimate: I_{L0}, I_{O0}, E_{g0}, R_{SH0}, and R_{S0}. The CEC model calibration techniques used in this study are described in detail in [15] and are briefly outlined here. The remaining parameters are determined in a two-step estimation

process: first, values of I_L, I_0, R_S, and R_{SH} are determined for each IV curve, then I_{L0}, I_{O0}, E_{g0}, R_{SH0}, and R_{S0} are determined by appropriate regressions developed from Eq. 6 through Eq. 10.

Calibration of the CEC model omits explicit accounting for reflection losses at the module's surface as is done with SAPM by the term f_2(AOI) in Eq. 1. We justify this omission by reasoning that except at very high angles-of-incidence the irradiance measured by a pyranometer fixed in the plane of the array is a reasonable value for the irradiance reaching a module's cells.

5 RESULTS

The calibrated SAPM and CEC models for each module were used to predict the out-of-sample data. For each model, POA irradiance and module back-surface temperature comprise the predictor variables. We computed I_{SC}, I_{MP}, V_{OC}, and V_{MP} using the SAPM and CEC calibrated models and compared the predictions with the measured values.

Figure 5 shows cumulative distribution functions (CDFs) for the absolute value of the difference between the predicted and measured P_{MP} values, expressed as a percentage of measured P_{MP}. Except for the tandem a-Si module predicted with the CEC model, P_{MP} prediction error is well below 10% for 90% of the data. For the SAPM, this level of prediction accuracy is comparable to, although somewhat less than, what is observed for module performance models calibrated using data obtained using a two-axis tracker [4, 5]. For the CEC model, prediction errors here are comparable to what is observed for data measured indoors on a flash tester [5]. The greater prediction errors for the CEC model applied to the tandem a-Si module are not surprising, given that this module is effectively a two-junction device, whereas the CEC model represents the module as a single diode equivalent circuit.

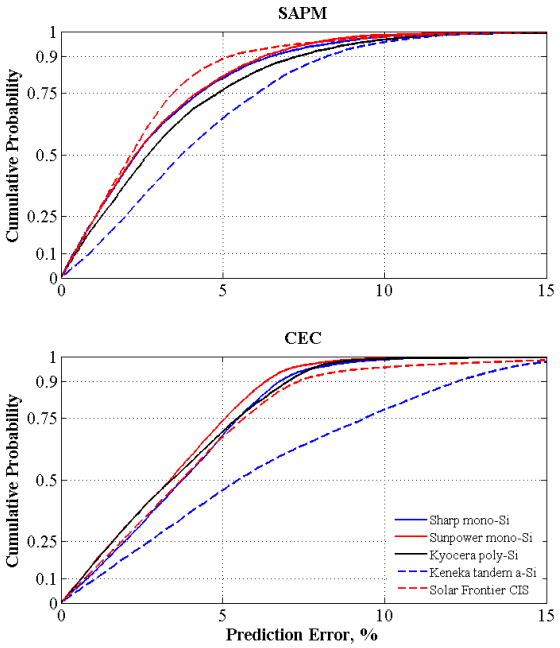

Figure 5: P_{MP} prediction error CDF for each module using the SAPM (top) and the CEC model (bottom).

Figure 6 plots the difference between predicted and measured P_{MP} over the range of POA irradiance. The scatterplots show that prediction error appears generally random at any particular POA irradiance level, and the range of prediction error at any particular POA irradiance level is roughly proportional to the POA irradiance. Slight biases are evident, toward overprediction of power for SAPM and underprediction for the CEC model, for this module.

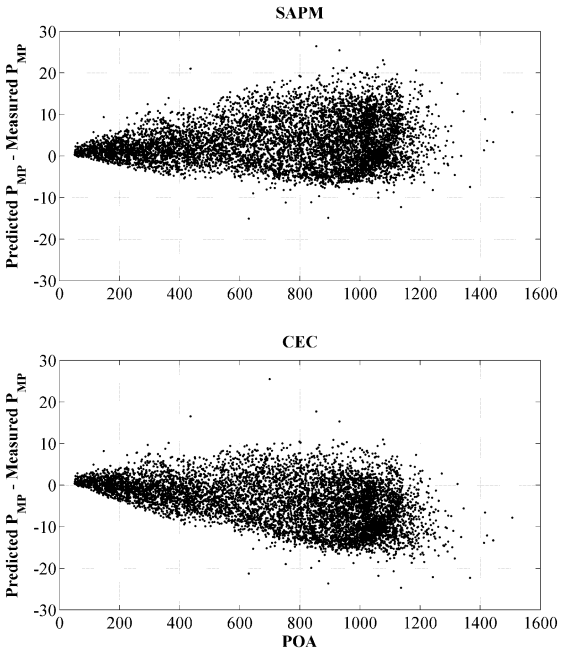

Figure 6: Prediction – Measured P_{MP} plotted with respect to POA using the SAPM (top) and CEC model (bottom) for the Kyocera poly-Si (235W) module.

6 CONCLUSIONS

In this paper, we have demonstrated that monitored system data can be used to calibrate reasonably accurate models for predicting output from PV modules. For a variety of module technologies and for both the SAPM and CEC models, prediction error for P_{MP} is generally within 10% of measured power over a wide range of conditions when the models are calibrated using monitored system data. These prediction errors are roughly twice as great as the prediction errors for models calibrated for data obtained outdoors using a two-axis tracker, or indoors using a solar simulator.

The calibration methods presented here use temperature coefficients from module data sheets rather than measured values. We believe that model prediction errors can be reduced substantially to be comparable to those from models calibrated using two-axis tracker or solar simulator data, if measured temperature coefficients are used rather than assuming datasheet values, and the techniques for accounting for solar spectrum effects are improved.

ACKNOWLEDGEMENT

Sandia National Laboratories is a multi-program laboratory managed and operated by Sandia Corporation, a wholly owned subsidiary of Lockheed Martin

Corporation, for the U.S. Department of Energy's National Nuclear Security Administration under contract DE-AC04 94AL85000. SAND Number 2014-17798 C

REFERENCES

[1] King, D. L., Boyson, E.E., Kratochvil, J.A. (2004). Photovoltaic Array Performance Model, Albuquerque, NM, Sandia National Laboratories.

[2] De Soto, W., Klein, S.A., Beckman, W.A. (2006). Improvement and validation of a model for photovoltaic array performance, *Solar Energy*, 80(1), 78-88.

[3] PVsyst, http://www.pvsyst.com

[4] Hansen, C., Stein, J., Miller, S., Boyson, E. E., Kratochvill, J. A., King, D. L. (2011). Parameter Uncertainty in the Sandia Array Performance Model for Flat-Plate Crystalline Silicon Modules, IEEE Photovoltaics Specialists Conference, Seattle, WA.

[5] Hansen, C., Riley, D., Jaramillo, M. (2012). Calibration of the Sandia Array Performance Model Using Indoor Measurements, IEEE Photovoltaic Specialists Conference, Austin, TX.

[6] Hansen, C. W, Luketa-Hanlin, A., Riley, D.A. (2013). Sensitivity of Single Diode Models for Photovoltaic Modules to Method Used for Parameter Estimation, 28th EU PVSEC, Paris, France.

[7] Dobos, A. (2012). An Improved Coefficient Calculator for the California Energy Commission 6 Parameter Photovoltaic Module Model, *J. Sol. Energy Eng*. 134(2).

[8] Haurwitz, B. (1945). Insolation in Relation to Cloudiness and Cloud Density, *Journal of Meteorology*, 2, 154-166.

[9] Perez, R., Ineichen, P., Maxwell, E., Seals, R., Zelenka, A. (1992). Dynamic Global-to-Direct Irradiance Conversion Models, ASHRAE Transactions-Research Series, pp. 354-369.

[10] PV_LIB, http://pvpmc.org/pv-lib/

[11] Loutzenhiser, P. G., Manz, H., Felsmann, C., Strachan, P. A., Frank, T., Maxwell, G. M. (2007). Empirical validation of models to compute solar irradiance on inclined surfaces for building energy simulation. *Solar Energy*, 81(2), 254-267.

[12] Reno, M.J., Hansen, C.W., Stein, J.S. (2012), Global Horizontal Irradiance Clear Sky Models: Implementation and Analysis, Albuquerque, NM, Sandia National Laboratories.

[13] Erbs, D.G., Klein, S.A., Duffie, J.A. (1982). Estimation of the diffuse radiation fraction for hourly, daily and monthly-average global radiation, *Solar Energy*, 28(4), 293-302.

[14] Martin, N., Ruiz, J. M. (2002), A New Model for PV Modules Angular Losses Under Field Conditions, *International Journal of Solar Energy*, 22(1), 19-31.

[15] Hansen, C. W. (2013). Estimation of Parameters for Single Diode Models Using Measured IV Curves. 39th IEEE Photovoltaic Specialists Conference, Tampa, FL.